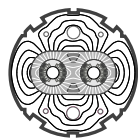


EUROPEAN ORGANIZATION FOR NUCLEAR RESEARCH
European Laboratory for Particle Physics



Large Hadron Collider Project

LHC Project Report 166

Electron Cloud in the LHC

Francesco Ruggiero*

Abstract

A theoretical and experimental crash program has been set up at CERN to investigate electron cloud effects in the LHC. In particular, I report about recent estimates of the critical secondary-emission yield, versus bunch population and bunch spacing, and ongoing multipacting tests with a coaxial resonator in a strong magnetic field.

Presented at the Advanced ICFA Workshop on *Beam Dynamics Issues for e^+e^- Factories*,
Laboratori Nazionali di Frascati - INFN, 20-25 October 1997, Frascati (Rome) - Italy

*CERN-SL Division

Administrative Secretariat
LHC Division
CERN
CH-1211 Geneva 23
Switzerland

Geneva, 4 February 1998

1 Introduction

Synchrotron radiation from proton bunches in the LHC creates photoelectrons at the beam screen wall. These photoelectrons are pulled towards the positively charged bunch. When they hit the opposite wall, they generate secondary electrons which can in turn be accelerated by the next bunch if they are slow enough to survive. Depending on several assumptions about surface reflectivity, photo-emission and secondary-emission yields, this mechanism can lead to the fast build-up of an electron cloud with potential implications for beam stability and heat load on the cold beam screen. In view of the tight deadline for the design of the LHC cryogenic system, an intensive research program [1] has been set up at CERN to measure the relevant physical quantities and to validate analytic estimates and simulation results.

The linear photon flux due to synchrotron radiation in the LHC is

$$\Phi_\gamma = \frac{5}{2\sqrt{3}} \alpha \gamma \frac{N_b}{\rho t_{\text{sep}}} \simeq 10^{17} \frac{\text{photons}}{\text{m} \cdot \text{s}}, \quad (1)$$

where $\alpha \simeq 1/137$ is the fine structure constant, $\gamma \simeq 7000$ the Lorentz factor for protons at 7 TeV, $N_b = 10^{11}$ the bunch population, $\rho \simeq 2780$ m the bending radius and $t_{\text{sep}} = 25$ ns the time separation between subsequent bunches. The critical energy of these photons is $\varepsilon_{\text{cr}} = 3/2 \gamma^3 \hbar c / \rho \simeq 45$ eV, i.e., well above the work function for copper (a few eV); photoelectrons are thus created at the beam screen wall and pulled towards the positively charged proton bunch. A first estimate [3] of the corresponding heat load on the beam screen, based on a photoelectron yield $\delta_{\gamma_e} \simeq 0.02$ and an average energy gain from the proton bunch $\langle W \rangle \simeq 700$ eV (in the absence of magnetic field and for a uniform electron cloud distribution), gave a linear power $P = \Phi_\gamma \delta_{\gamma_e} \langle W \rangle \simeq 0.2$ W/m comparable to the heat load due to synchrotron radiation. This estimate does not include a possible electron cloud build-up associated with secondary emission, which can significantly increase the power deposition and, according to earlier simulations [2], can lead to a very fast horizontal multi-bunch instability.

For a uniform illumination of the beam screen, corresponding to high surface reflectivity, the average energy gain in a dipole magnet is smaller by a factor two, since only the vertical component of the beam force is effective in accelerating the electrons. Indeed they spiral along the vertical magnetic field lines with typical Larmor radii of a few μm and perform about a hundred cyclotron rotations during a bunch passage. On the other hand, the heat load in a dipole magnet is drastically reduced if the screen reflectivity is much smaller than unity: in this case, photoelectrons and secondary electrons are produced only near the horizontal plane, where the vertical component of the beam force is very small.

For high surface reflectivity, the measured photoelectron yield per *incident* photon may differ significantly from the relevant yield per *absorbed* photon (sooner or later all photons are absorbed by the beam screen). Therefore simultaneous measurements of photoelectron yield and reflectivity, at grazing incidence angle of 11 mrad, are under way at CERN using synchrotron light from the EPA machine, with critical energy of 45 eV. Recent results [4] for copper coatings with different surface preparations indicate a rather high photoelectron yield per absorbed photon $\delta_{\gamma_e} \simeq 0.15 \div 0.20$, however the reflectivity drops from 80% for smooth surfaces down to about 5% for a surface roughness of a few μm .

In kick approximation, the maximum energy gain of an electron initially at rest with radial offset a from the beam axis is independent of the bunch length and given by $\varepsilon_{\text{max}} = 2m_e c^2 N_b^2 r_e^2 / a^2$, where c is the speed of light, m_e the electron mass and r_e

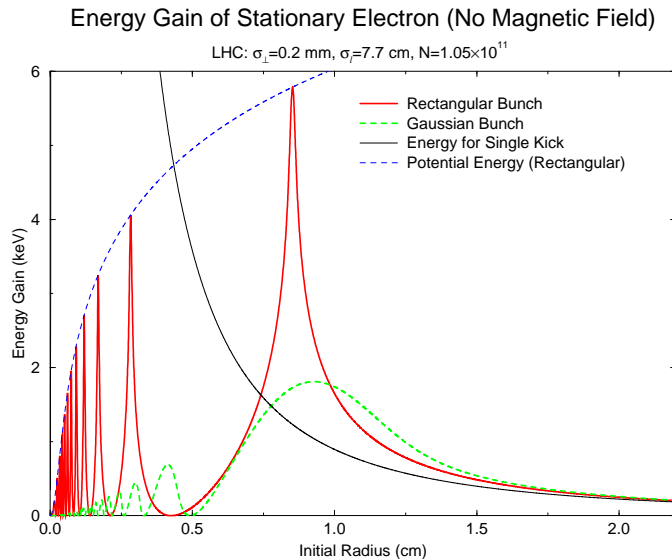


Figure 1: Electron energy gain (keV) versus initial radial offset (cm) for the LHC: the solid curve diverging at small radial offsets is the kick approximation, the two lower curves refer to Gaussian and rectangular longitudinal bunch distributions. Here the peaks correspond to electrons temporarily trapped in the bunch potential, performing an integer number of oscillations plus one quarter [5].

its classical radius. For a photoelectron starting at the wall $a \simeq 2$ cm of the LHC beam screen, $\varepsilon_{\max} \simeq 200$ eV and the corresponding travel time to the opposite wall is about 5 ns, i.e., significantly less than the 25 ns bunch spacing. When the next bunch arrives, there is a relatively uniform distribution of photoelectrons (plus secondary electrons) in the screen cross section: the energy gain can reach a few keV and these fast particles hit very quickly the screen walls, producing low energy secondary electrons. However, for a correct modelling of the electron motion during the bunch passage [5] one has to cut the bunch into several transverse slices (typically 50). This is important for electrons near the beam axis, when the energy gain in kick approximation is largely overestimated (see Fig. 1), and is a key ingredient in all recent simulations of the electron cloud dynamics [6, 7, 8].

2 Electron cloud build-up and critical secondary electron yield

Here I shortly review the theory of electron cloud build-up recently developed at CERN by G. Stupakov [9] and use his quasi-analytic results to discuss the dependence of the critical secondary emission yield δ_{cr} on the bunch population N_b and bunch separation $L_{\text{sep}} = ct_{\text{sep}}$.

The average number of secondary electrons emitted when a primary electron of energy W hits a metal surface with incidence angle θ from the normal can be written [10]

$$\delta_{\text{SEY}}(W, \theta) = \frac{\delta_{\max}}{\cos \theta} h\left(\frac{W}{W_o}\right), \quad (2)$$

where the maximum yield δ_{\max} , corresponding to a primary electron energy W_o typically around 400 eV, is a characteristic of the metal ($\delta_{\max} = 1.3 \div 2.5$ for copper, depending on surface preparation), while h is a universal function having the following phenomenological expression:

$$h(\xi) = 1.11 \xi^{-0.35} \left(1 - e^{-2.3 \xi^{1.35}}\right). \quad (3)$$

With some simplifying assumptions about the shape of the beam screen (circular with radius a) and the velocity distribution of the secondary electrons (half-Maxwellian with characteristic energy $W_s = mv_s^2$), it is possible to solve analytically the Vlasov equation describing the free drift of these electrons along the vertical magnetic field lines in a bending dipole. The initial phase space distribution for secondary electrons produced at the screen wall with vertical coordinate $y_o(x) = \sqrt{a^2 - x^2}$ is

$$f_e^{(o)}(x, y, v) = n_o(x) \sqrt{\frac{2m}{\pi W_s}} e^{-mv^2/2W_s} \delta(y \pm y_o(x)), \quad (4)$$

where $n_o(x)$ denotes the initial electron surface density at the screen wall projected on the horizontal plane (particles per unit area in the horizontal plane) and the velocity $v > 0$ is directed from the wall towards the beam axis. The vertical drift velocity along the magnetic field lines is $v_y = \mp v y_o/a$ and the evolution of the electron cloud density $n_e(x, y, t)$ during the time interval between two subsequent bunches is given by

$$n_e(x, y, t) = \frac{2n_o(x)}{tv_s y_o(x)/a} \left[\lambda \left(\frac{y - y_o(x)}{tv_s y_o(x)/a} \right) + \lambda \left(\frac{y + y_o(x)}{tv_s y_o(x)/a} \right) \right], \quad (5)$$

where $\lambda(\xi) = (1/\sqrt{2\pi}) \exp(-\xi^2/2)$ and the two terms in square brackets account for electrons drifting away from the upper or lower parts of the screen walls, respectively. Combining the energy gain from the next bunch $W(x, y) = \varepsilon_{\max} a^2 y^2 / (x^2 + y^2)^2$, in kick approximation and in presence of a vertical magnetic field, with the secondary electron yield given by Eq. (2), one gets the ‘second generation’ electron surface density

$$n_1(x) = \int_{-y_o(x)}^{y_o(x)} dy \delta_{\text{SEY}}(W(x, y), \theta(x)) n_e(x, y, t_{\text{sep}}). \quad (6)$$

Here $\theta(x) = \arccos(y_o(x)/a)$. Although the kick approximation fails for electron energies larger than about 1 keV, the corresponding secondary emission is a smooth function of W at such energies and the error is not expected to be significant. Note that Eq. (6) is valid assuming that the surviving first generation electrons hit the screen wall instantaneously after the passage of the next bunch.

Build-up of the electron cloud will take place if $n_1(x) > n_o(x)$, i.e., if $\delta_{\max} > \delta_{\text{cr}}(x)$ where

$$\delta_{\text{cr}}(x) = \left\{ \int_{-y_o(x)}^{y_o(x)} dy h(W(x, y)) \frac{a}{y_o(x)} \frac{n_e(x, y, t_{\text{sep}})}{n_o(x)} \right\}^{-1}. \quad (7)$$

This defines a critical value δ_{cr} , weakly dependent on the horizontal position x along the beam screen cross section, for the maximum secondary electron yield: if δ_{\max} is smaller than the critical value, there is no spontaneous amplification of the electron cloud density.¹⁾ For nominal LHC parameters ($N_b = 10^{11}$, $L_{\text{sep}} = 7.5$ m) and assuming a typical secondary electron energy $W_s = 10$ eV, one finds a minimum δ_{cr} of about 1.35, in agreement with simulation results [8]. Such a low value for δ_{\max} is not easy to achieve. As shown in Fig. 2, however, δ_{cr} increases significantly for larger bunch spacings and has a weak dependence on the bunch population. Therefore, as a possible back-up solution, one could envisage to double the LHC bunch spacing.

¹⁾ The definition of δ_{cr} does not include space charge effects, which can be neglected at the beginning of the electron cloud build-up. An approximate analytic solution of the Vlasov equation is possible, however, even including space charge [9]. It would be interesting to extend this approach to take into account the effect of the resistive wall wakefield, which might play a significant role during the inter-bunch gaps.

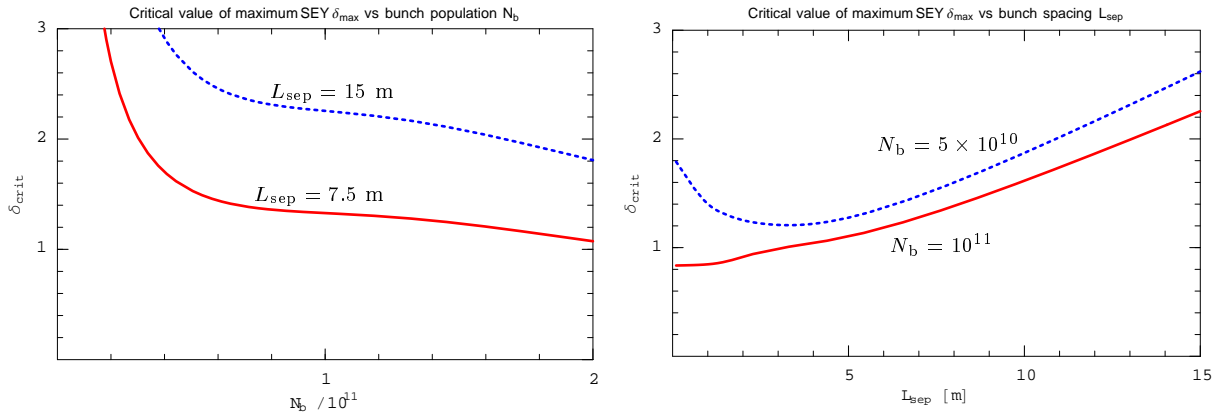


Figure 2: Minimum value of the critical secondary electron yield given by Eq. (7), for a circular screen of radius $a = 2$ cm and a secondary electron energy $W_s = 10$ eV, versus bunch population (left) and bunch spacing (right). The solid and dotted curves correspond to a bunch spacing of 7.5 m and 15 m (left) or to a bunch population of 10^{11} and 5×10^{10} (right), respectively.

3 Multipacting tests

The secondary electron yield and its possible reduction by a strong dipole magnetic field can be inferred from the multipacting level reached under suitable conditions in a resonant coaxial setup. Measurements of photoelectron yield and of multipacting rise time may also be possible using UV light (e.g., from a Xe flash lamp mounted near or inside the coaxial tube) and applying a DC-voltage between inner and outer conductors of the coaxial structure. Comparing experimental results and predictions of computer simulations will also provide a very useful ‘calibration’ for the numerical results concerning heat load on the LHC beam screen.

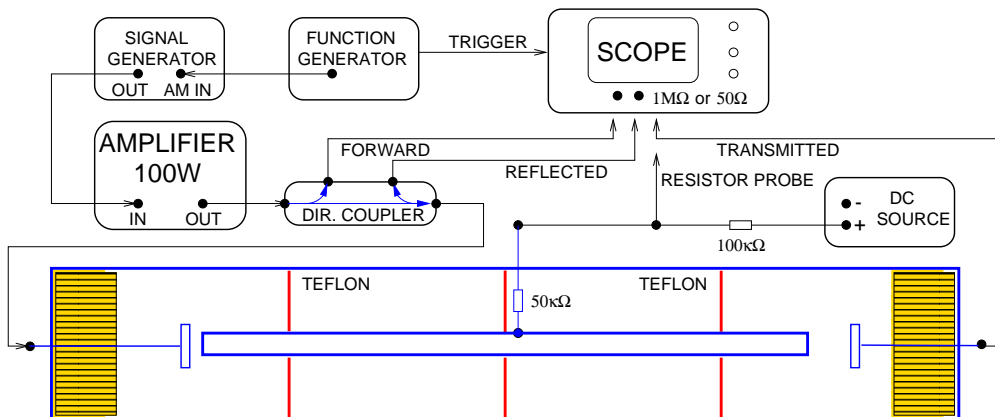


Figure 3: Experimental setup for multipacting tests. Using a coaxial resonator we can reach high electric fields and RF-voltages between the inner and outer conductor, in spite of the limited power of the wide-band amplifier: for a Q of 1000 and a characteristic impedance of about 100Ω , a power of 100 W corresponds to a peak voltage of $\sqrt{100 \text{ W} \times 100 \Omega \times 1000} \simeq 3 \text{ kV}$.

Multipacting tests have been successfully performed at CERN [11] using the coaxial setup shown in Fig. 3. We have developed a simple and reliable technique, based on amplitude modulation of the input signal, to detect electronically the onset of multipacting

and to monitor the field level in the resonator. An example of multipacting signature is shown in Fig. 4a: no reflected signal (upper trace) is present until the amplitude modulated input signal reaches a threshold value. Meanwhile the transmitted signal (lower trace) increases and then becomes constant in the multipacting range. We observe a negative low-frequency signal superimposed on the ‘resistor probe’ RF signal from the inner conductor, as in the lower trace of Fig. 4b, and thus the electric potential of the inner conductor tends to become negative during multipacting. Although the sign of this low-frequency signal becomes positive with a strong magnetic field, as shown in Fig. 4c, the multipacting thresholds at room temperature are qualitatively similar to those measured during recent cold tests, with a dipole magnetic field up to about 7.5 T. This seems to exclude any significant reduction of the secondary electron yield by a strong magnetic field over most of the outer tube surface, where the field is not strictly parallel to the metal.

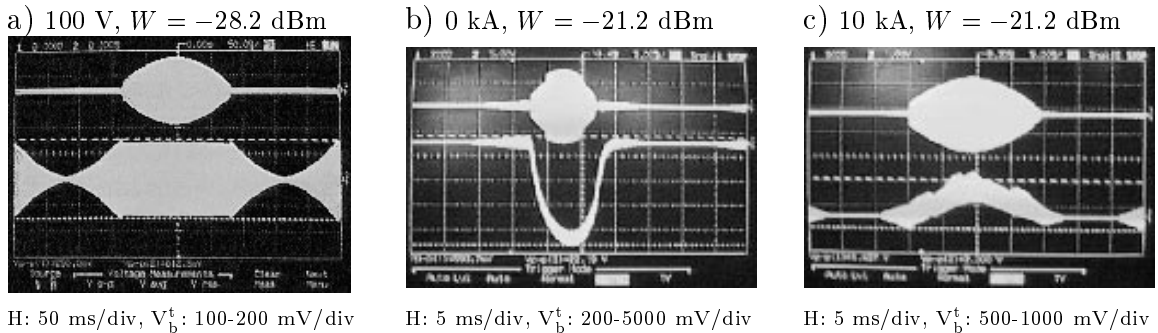


Figure 4: Multipacting tests in a resonant coaxial setup: with 100 V DC-bias and no magnetic field (a), in a cryostat at 1.8 K without magnetic field (b) and with a dipole field of 7.3 T (c). The generator signal, with frequency around 480 MHz and power W , is amplitude modulated at 3 Hz (a) or at 30 Hz (b)-(c) and amplified at maximum gain (~ 60 dB). The upper trace is the reflected signal attenuated by 40 dB and measured with a 50Ω load, the lower trace is the transmitted signal (a) or the ‘resistor probe’ signal (b)-(c) measured with a $1 \text{ M}\Omega$ load.

References

- [1] F. Ruggiero, World-wide web page on *Electron Cloud in the LHC*, <http://wwwslap.cern.ch/collective/electron-cloud/>.
- [2] F. Zimmermann, *A Simulation Study of Electron-Cloud Instability and Beam-Induced Multipacting in the LHC*, CERN LHC Project Report 95 (1997).
- [3] O. Gröbner, *Beam Induced Multipacting*, CERN LHC Project Report 127 (1997), presented at the IEEE Particle Accelerator Conference, Vancouver, 1997.
- [4] I.R. Collins and O. Gröbner, private communication (October 1997).
- [5] J.S. Berg, *Energy Gain in an Electron Cloud During the Passage of a Bunch*, CERN LHC Project Note 97 (1997).
- [6] F. Zimmermann, *Electron-Cloud Instability and Beam-Induced Multipacting in the LHC and in the VLHC*, SLAC-PUB-7664 (1997), presented at the workshop MBI’97, KEK, Tsukuba, Japan, 1997 and contributions to these proceedings.
- [7] M.A. Furman, *Comments on the Electron-Cloud Effect in the LHC Dipole Bending Magnets*, LBNL 40914/CBP Note-241 (1997), presented at the workshop MBI’97, KEK, Tsukuba, Japan, 1997 and contributions to these proceedings.

- [8] O. Brüning, *Simulations for the Beam-induced Electron Cloud in the LHC liner*, CERN LHC Project Note 102 and LHC Project Report 158 (1997).
- [9] G. Stupakov, *Photoelectrons and Multipacting in the LHC: Electron Cloud Build-up*, CERN LHC Project Report 141 (1997).
- [10] H. Seiler, *Secondary electron emission in the scanning electron microscope*, J. Appl. Phys. **54**, 11 (1983).
- [11] F. Caspers, J.-M. Laurent, M. Morvillo, and F. Ruggiero, *Multipacting tests with a resonant coaxial setup*, CERN LHC Project Note 110 (1997).